OPEN

A PrP^C-caveolin-Lyn complex negatively controls neuronal GSK3β and serotonin 1B receptor

Julia Hernandez-Rapp[1,2,3]*, Séverine Martin-Lannerée[1,2]*, Théo Z. Hirsch[1,2]*, Elodie Pradines[1,2], Aurélie Alleaume-Butaux[1,2], Benoît Schneider[1,2], Anne Baudry[1,2], Jean-Marie Launay[4,5] & Sophie Mouillet-Richard[1,2]

[1]INSERM UMR-S1124, 75006 Paris France, [2]Université Paris Descartes, Sorbonne Paris Cité, UMR-S1124, 75006 Paris France, [3]Université Paris Sud 11, ED419 Biosigne, 91400 Orsay, France, [4]AP-HP Service de Biochimie, Fondation FondaMental, INSERM U942 Hôpital Lariboisière, 75010 Paris, France, [5]Pharma Research Department, F. Hoffmann-La-Roche Ltd., CH-4070 Basel, Switzerland.

The cellular prion protein, PrP^C, is a glycosylphosphatidylinositol-anchored protein, abundant in lipid rafts and highly expressed in the brain. While PrP^C is much studied for its involvement under its abnormal PrP^{Sc} isoform in Transmissible Spongiform Encephalopathies, its physiological role remains unclear. Here, we report that GSK3β, a multifunctional kinase whose inhibition is neuroprotective, is a downstream target of PrP^C signalling in serotonergic neuronal cells. We show that the PrP^C-dependent inactivation of GSK3β is relayed by a caveolin-Lyn platform located on neuronal cell bodies. Furthermore, the coupling of PrP^C to GSK3β potentiates serotonergic signalling by altering the distribution and activity of the serotonin 1B receptor (5-HT$_{1B}$R), a receptor that limits neurotransmitter release. In vivo, our data reveal an increased GSK3β kinase activity in PrP-deficient mouse brain, as well as sustained 5-HT$_{1B}$R activity, whose inhibition promotes an anxiogenic behavioural response. Collectively, our data unveil a new facet of PrP^C signalling that strengthens neurotransmission.

T he cellular prion protein PrP^C, whose conversion into its scrapie isoform PrP^{Sc} causes prion diseases, is a ubiquitous, glycosylphosphatidylinositol (GPI)-anchored glycoprotein predominantly expressed in neurons[1]. Despite intense research, our knowledge of the biological function of PrP^C still is far from complete. Recently, increasing attention has been paid to the involvement of PrP^C in signal transduction, especially since PrP^C appears to act as a receptor for the beta-amyloid peptide Aβ and to mediate Aβ neurotoxicity[2,3]. PrP^C can indeed recruit signalling cascades after engagement with partners, which, beyond Aβ, include PrP^C itself[4] or the protective factor STI-1[5,6]. Such interactions can be mimicked through antibody-mediated ligation of PrP^C [7,8]. By exploiting the later strategy and the 1C11 cell line with its differentiated serotonergic (1C11^{5-HT}) or noradrenergic (1C11^{NE}) neuronal progenies[9], we previously identified neurospecific PrP^C-dependent signalling pathways, under the control of a signalling platform where PrP^C associates with caveolin and the Fyn kinase. While PrP^C, caveolin and Fyn are present in both cell bodies and neuronal processes, their association within a signalling complex is spatially restricted to the neurites of differentiated cells[7], raising the issue of potential signal transduction cascades imparted by PrP^C species located on the cell bodies. We further identified effectors downstream this complex, including NADPHoxidase and CREB, which support an involvement of PrP^C in neuronal survival and plasticity[8,10].

Another important gatekeeper of neuronal homeostasis is the Glycogen Synthase Kinase 3β (GSK3β) multifunctional serine/threonine kinase[11]. Unlike most kinases, GSK3β is active under resting conditions and is primarily regulated through inhibition. Its activity is facilitated by phosphorylation on Tyrosine 216 (Y216), which may notably occur through autophosphorylation, while phosphorylation on Serine 9 (S9) is sufficient to inhibit its kinase activity[12]. Inactivation of GSK3β occurs in many pathways, including Wnt, insulin and growth factors[13] and is associated with diverse aspects of neuronal function, such as the onset and maintenance of neuronal polarity, survival and activity[14]. On the opposite, GSK3β overactivation impairs neuronal architecture, plasticity and survival[12].

Here, we report that PrP^C instructs the phosphorylation of GSK3β on S9 in neuronal cells and that this response occurs after both antibody-mediated ligation of PrP^C or binding to its ligand STI-1. We show that the inhibition of GSK3β is imparted by full-length PrP^C species located on cell bodies, and is relayed by a Lyn kinase - phosphoinositide 3 kinase (PI3K) - Akt module, via caveolin. Our in vitro data further indicate that the mobilization of the PrP^C-GSK3β cascade cancels the activity of the serotonin 1B receptor (5-HT$_{1B}$R), a negative regulator of neurotransmitter release. Finally, we provide evidence for increased GSK3β and 5-HT$_{1B}$R activities in the brain of PrP-deficient mice, which correlate with neurochemical and behavioural changes.

Results

PrP^C promotes inactivation of GSK3β in 1C11^{5-HT} neuronal cells. To probe the occurrence of a signalling pathway linking PrP^C to GSK3β, we monitored the level of pS9-GSK3β and pY216-GSK3β in 1C11^{5-HT} neuronal cells exposed to PrP^C antibodies, a means to study PrP^C-dependent cell signalling events[7]. Because PrP^C is subject to proteolytic processing at position 111/112, we performed our experiments with antibodies directed against the N-terminus (SAF32), which recognize only full-length PrP^C, and antibodies against the C-terminus (SAF61), which target both full-length and truncated PrP^C species[15]. 1C11^{5-HT} cells expressed a basal level of pY216-GSK3β, which was barely sensitive to either PrP^C antibodies, within a 120 min time scale (Fig. 1a,b). In contrast, we found that PrP^C ligation with SAF32 antibodies, targeting native PrP^C only, induced a 160% increase in the level of pS9-GSK3β, which started after 5 min and persisted for 2 h

onwards (Fig. 1c). Of note, antibodies targeting a C-terminal epitope (SAF61) did not promote the phosphorylation of GSK3β on S9 (Fig. 1d).

In agreement, immunofluorescence analysis revealed a marked increase in the intensity of pS9-GSK3β signal following exposure of 1C11^{5-HT} serotonergic cells to SAF32 antibodies, which localized faintly on neuritic extensions and, most notably, on cell bodies (Fig. 1e). On the opposite, the pS9-GSK3β labeling in cells treated with SAF61 was similar to that of control 1C11^{5-HT} cells (Fig. 1e).

We further analyzed the status of p-GSK3β in PrP^C-depleted 1C11^{5-HT} cells. While the level of pY216-GSK3β was unaffected by siRNA-mediated knockdown of PrP^C, we monitored a drastic (84%) reduction in pS9-GSK3β in PrP^C-depleted 1C11^{5-HT} cells versus control cells (Fig. 1f), indicating that PrP^C depletion exacerbates basal GSK3β activity.

Next, we sought to evaluate the physiological relevance of the signalling events induced by antibody ligation by mimicking the interaction of PrP^C with its ligand STI-1[6]. To this purpose, 1C11^{5-HT} neuronal cells were exposed to a STI-1 peptide corresponding to the PrP^C binding domain, as in[6]. First, we observed that the binding of the STI-1 peptide to 1C11^{5-HT} cells was hindered by SAF32 antibodies in a dose-dependent manner (Fig. S1a), supporting the notion that the ligation of SAF32 antibody mimics the endogenous binding of STI-1 to PrP^C. As with SAF32-mediated PrP^C ligation, the STI-1 peptide had no effect on the level of pY216-GSK3β (Fig. 1g), while it induced a strong increase in the level of pS9-GSK3β (185%) (Fig. 1h). The levels of pS9-GSK3β and pY216-GSK3β were however insensitive to exposure to a scramble control peptide (Fig. S1b). Of
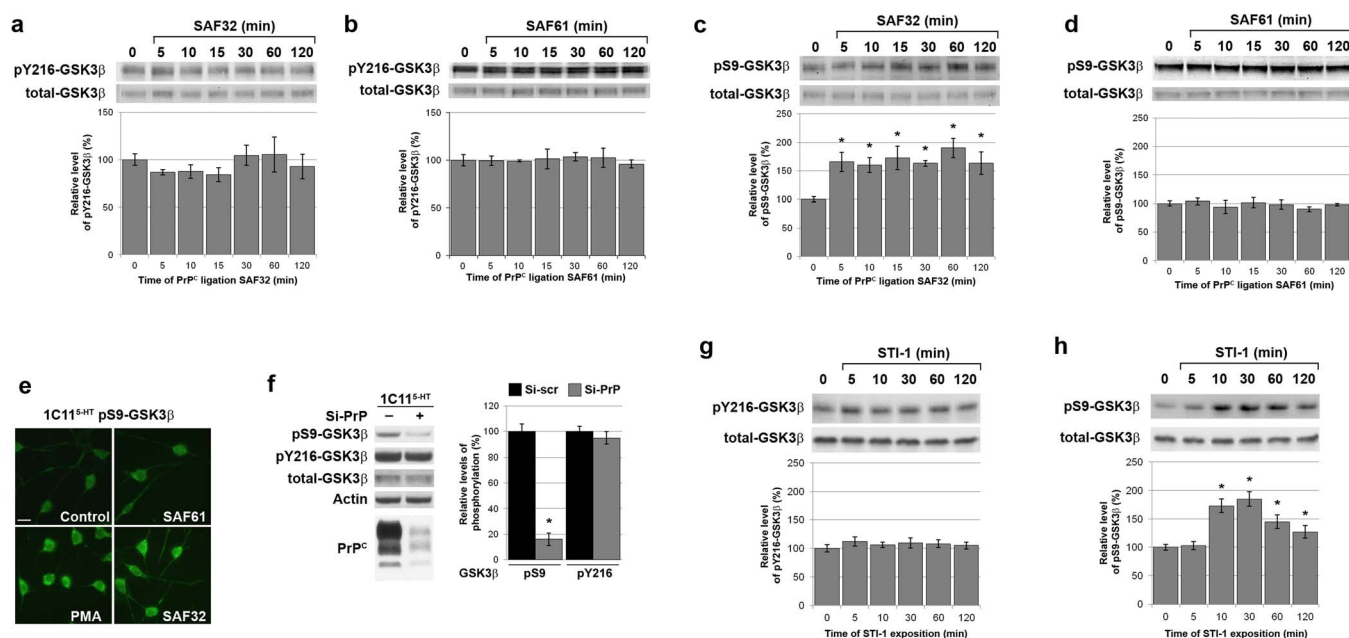
Figure 1 | Stimulation of native PrP^C promotes GSK3β phosphorylation on S9. (a–d) 1C11^{5-HT} neuronal cells were exposed to anti-PrP^C antibodies targeting a N-terminal epitope (SAF32, 10 μg/ml) (a), (c) or a C-terminal epitope (SAF61, 10 μg/ml) (b), (d). Cell lysates were immunoblotted with antibodies targeting either pY216-GSK3β (a), (b) or pS9-GSK3β (c), (d). Levels of pY216-GSK3β (a), (b) or pS9-GSK3β (c), (d) were normalized to total GSK3β for quantification. (e) 1C11^{5-HT} neuronal cells exposed to various anti-PrP^C antibodies (SAF32, SAF61, each 10 μg/ml) for 30 min were stained with anti pS9-GSK3β antibodies. Unstimulated cells and cells treated with the phorbol ester PMA (5 μM, 30 min), a known inducer of phosphorylation of GSK3β at S9[12], were included as negative and positive controls, respectively. Scale bar = 25 μm. (f) The levels of pS9-GSK3β, pY216-GSK3β and total GSK3β were assessed by immunoblotting in 1C11^{5-HT} cells transfected for 36 h with a siRNA targeted against PrP (Si-PrP) or a control scramble siRNA (Si-scr). immunoblotting with antibodies to PrP^C and actin was carried out to check knockdown and as loading control, respectively. (g), (h) 1C11^{5-HT} neuronal cells were exposed to a peptide corresponding to the domain of STI-1 that binds PrP^C (aa 230–245) (25 μM). Cell lysates were immunoblotted with antibodies targeting either pY216-GSK3β (g) or pS9-GSK3β (h). Levels of pY216-GSK3β (g) or pS9-GSK3β (h) were normalized to total GSK3β for quantification. Gels have been cropped for clarity and conciseness purposes; original images corresponding to (a–d) are shown in Supplemental Figure 4. All data are representative of a set of n = 4 to 6 independent experiments. Results are expressed as means ± S.E.M. *$P < 0.05$ vs. control, Kolmogorov-Smirnov test.

note, the occurence of the PrP^C-GSK3β coupling could be extented to PC12 cells. Indeed, exposure of differentiated PC12 cells to the STI-1 peptide promoted the phosphorylation of GSK3β at S9 (150%), while not affecting phosphorylation at Y216, in accordance with the data obtained with 1C11$^{5\text{-HT}}$ cells (Fig. S2).

These results introduce GSK3β as a novel target of PrP^C signalling in neuronal cells. They show that the phosphorylation of GSK3β on Y216 does not depend on PrP^C. In contrast, PrP^C can induce the phosphorylation of GSK3β on S9 and thereby limit its kinase activity. This inactivation of GSK3β is observed after ligation with antibodies targeting the N-terminal -but not the C-terminal- region of PrP^C. Of note, this coupling occurs endogenously and can be mobilized by the interaction of PrP^C with its natural ligand STI-1.

PrP^C negatively controls GSK3β in vivo. We then tested the occurrence of a PrP^C-GSK3β coupling in vivo. First, we observed a reduction in the level of pS9-GSK3β (19% of control levels), but not pY216-GSK3β, in brain extracts from PrP$^{0/0}$ mice as compared to their wild-type (WT) counterparts (Fig. 2a), in line with our in vitro results. Furthermore, in WT mice, the stereotaxic injection of SAF32 antibodies into the raphe nuclei, a brain cluster of serotonergic neurons, promoted a potent increase in pS9-GSK3β (187%), with a kinetics that globally compared that observed in vitro (Fig. 2b). In line with our in vitro data, the level of pY216-GSK3β was insensitive to SAF32 injection in the raphe of WT mice (Fig. 2c). Of note, SAF32 antibodies failed to induce any change in the levels of pS9-GSK3β (Fig. 2d) or pY216-GSK3β (Fig. 2e) in the raphe of PrP$^{0/0}$ mice. Finally, as with 1C11$^{5\text{-HT}}$ cells, the injection of SAF61 antibodies into the raphe of WT mice did not impact on the level of either pS9-GSK3β (Fig. 2f) or pY216-GSK3β (Fig. 2g). Collectively, these data provide an in vivo validation of the PrP^C coupling to GSK3β.

The PrP^C coupling to GSK3β is controlled by the Lyn kinase via caveolin-1. Next, we searched for intermediates linking PrP^C to GSK3β. Previously, we identified the src kinase Fyn as a downstream target of PrP^C signalling in 1C11$^{5\text{-HT}}$ neuronal cells[7]. However, we found no significant impact of Fyn blockade on the increase in pS9-GSK3β promoted by SAF32 antibodies (Fig. 3a). A good candidate alternative to Fyn for relaying the inactivation of GSK3β is Lyn, another src kinase, which partitions with PrP^C in rafts of neuronal cells[16]. The level of pY507-Lyn, which corresponds to inactivated Lyn[17], did not vary when 1C11$^{5\text{-HT}}$ neuronal cells were exposed to the C-terminal SAF61 antibody (Fig. 3b). In contrast, we observed a decrease (58%) in the level of pY507-Lyn 5 min following SAF32 antibodies addition, onwards (Fig. 3c), indicating an activation of the Lyn kinase. Of note, exposure of 1C11$^{5\text{-HT}}$ neuronal cells to the STI-1 peptide induced a similar (66%) decrease in pY507-Lyn, revealing Lyn activation (Fig. 3d). A comparable decrease in pY507-Lyn was observed in PC12 differentiated cells in response to the STI-1 peptide (Fig. S2).

To determine whether Lyn indeed relays the PrP^C-GSK3β coupling, 1C11$^{5\text{-HT}}$ neuronal cells were transfected with a siRNA against Lyn prior to exposure to SAF32 antibodies. The knockdown of Lyn fully reduced the basal level of pS9-GSK3β (4%) and blunted the PrP^C-dependent increase in pS9-GSK3β (Fig. 3e). In contrast, the level of pY216-GSK3β remained intact in Lyn-depleted cells (Fig. 3e). Then, we probed an involvement of the membrane protein caveolin-1 in the PrP^C-Lyn coupling, since caveolin-1 interacts with both PrP^C [7] and Lyn[18]. Of note, the SAF32-induced dephosphorylation of Lyn at Y507 was cancelled under immunosequestration of caveolin-1 (Fig. 3f). Finally, while Lyn did not interact with PrP^C under basal conditions, it co-immunoprecipitated with PrP^C in cells exposed to the STI-1 peptide or SAF32 antibodies (Fig. 3g). Altogether, these data support the occurrence of a PrP^C-caveolin-Lyn signalling complex in 1C11$^{5\text{-HT}}$ neuronal cells, which drives the

PrP^C-induced inactivation of GSK3β and can be mobilized by STI-1, an endogenous ligand of PrP^C.

The PrP^C-Lyn-GSK3β cascade is mediated by prion proteins located on cell bodies of 1C11$^{5\text{-HT}}$ neuronal cells. All signal transduction cascades that we identified previously in 1C11$^{5\text{-HT}}$ cells are imparted by neuritic PrP^C and rely on the PrP^C-caveolin-Fyn platform implemented on the neurites, although PrP^C, caveolin and Fyn are present both in cell bodies and neuronal processes of these serotonergic cells[7,8]. Here, the GSK3β phosphorylation on S9 in response to SAF32 antibodies is independent from Fyn but depends on Lyn activation. In addition, this signal is mainly observed at the cell bodies in immunofluorescence (Fig. 1e). We thus assessed a potential spatial restriction of the PrP^C-Lyn-GSK3β cascade by separating cell bodies from neurites of 1C11$^{5\text{-HT}}$ neuronal cells prior to exposure to anti-PrP^C antibodies. While Lyn was detected in both fractions, we observed a SAF32-dependent decrease in pY507-Lyn in the fraction enriched in cell bodies only (Fig. 4a). As anticipated, the status of Lyn was insensitive to SAF61 antibodies, whether in the cell bodies or in the neurites (Fig. 4b). Accordingly, the SAF32-mediated phosphorylation of GSK3β at S9 was restricted to the cell bodies fraction (Fig. 4c). As with Lyn, total GSK3β however distributed in both cell bodies and neurites (Fig. 4c). Thus, while PrP^C, Lyn and GSK3β are present in both cell bodies and neuronal processes, the PrP^C-Lyn-GSK3β cascade is spatially restricted to the cell bodies of 1C11$^{5\text{-HT}}$ neuronal cells. This observation raises the question as to the selective recruitment of Lyn or Fyn by PrP^C molecules located on the cell bodies or the neurites, respectively. Because these two src kinases are differentially palmitoylated and may partition in different membrane compartments[18], we probed their association with the plasma membrane in relation with their distribution in cell bodies versus neurites. The plasma membrane fraction of Lyn was majorly found in the cell bodies (79% of total membrane-associated Lyn), while, conversely, the plasma membrane fraction of Fyn was predominantly found in the neurites (82% of total membrane-associated Fyn) (Fig. 4d). Thus, the spatial control of Lyn membrane association appears to drive the selective implementation of the PrP^C-caveolin-Lyn platform in the cell bodies of 1C11$^{5\text{-HT}}$ neuronal cells, and may therefore account for the restriction of the PrP^C-GSK3β cascade to the somatic compartment.

The PrP^C-GSK3β cascade in 1C11$^{5\text{-HT}}$ neuronal cells is controlled by PI3K and Akt downstream from Lyn and involves copper and LRP1. Next, we sought to identify potential intermediate effector(s) relaying the inactivation of GSK3β downstream from Lyn. Because Lyn can phosphorylate the p85 subunit of PI3K (Y458) in erythroid cells[17] and in view of the classical PI3K-Akt-GSK3β pathway[11], we probed an involvement of the PI3K-Akt module. As anticipated, exposure of 1C11$^{5\text{-HT}}$ neuronal cells to the PI3K inhibitor wortmannin or to the Akt inhibitor MK-2206 did not affect the SAF32-induced decrease in pY507-Lyn (Fig. 5a,b). In contrast, siRNA-mediated silencing of Lyn blunted the SAF32-induced phosphorylation of p85-PI3K at Y458 (Fig. 5c). Furthermore, both wortmannin and MK-2206 cancelled the increase in pS9-GSK3β in response to SAF32 antibodies (Fig. 5d,e), indicating that the PI3K-Akt module mediates the PrP^C-GSK3β coupling downstream from Lyn in 1C11$^{5\text{-HT}}$ neuronal cells.

Interestingly, PI3K activity has been reported to be stimulated by native, but not N-terminally truncated, PrP^C [19]. A hallmark of the N-terminal region of PrP^C is the presence of octapeptide repeats that have the capacity to bind up to four copper ions Cu^{2+} [20]. The SAF32 epitope precisely maps in the copper-binding octapeptide region of PrP^C [15]. In the supernatant of 1C11$^{5\text{-HT}}$ cells, we measured a free Cu^{2+} concentration of 0.21 μM, suggesting that the N-terminus of cell-surface PrP^C is copper-bound in these neuronal cells[20]. We thus examined the impact of copper chelation on the PrP^C-Lyn-PI3K-GSK3β coupling. Pre-incubation with the copper chelator D-peni-
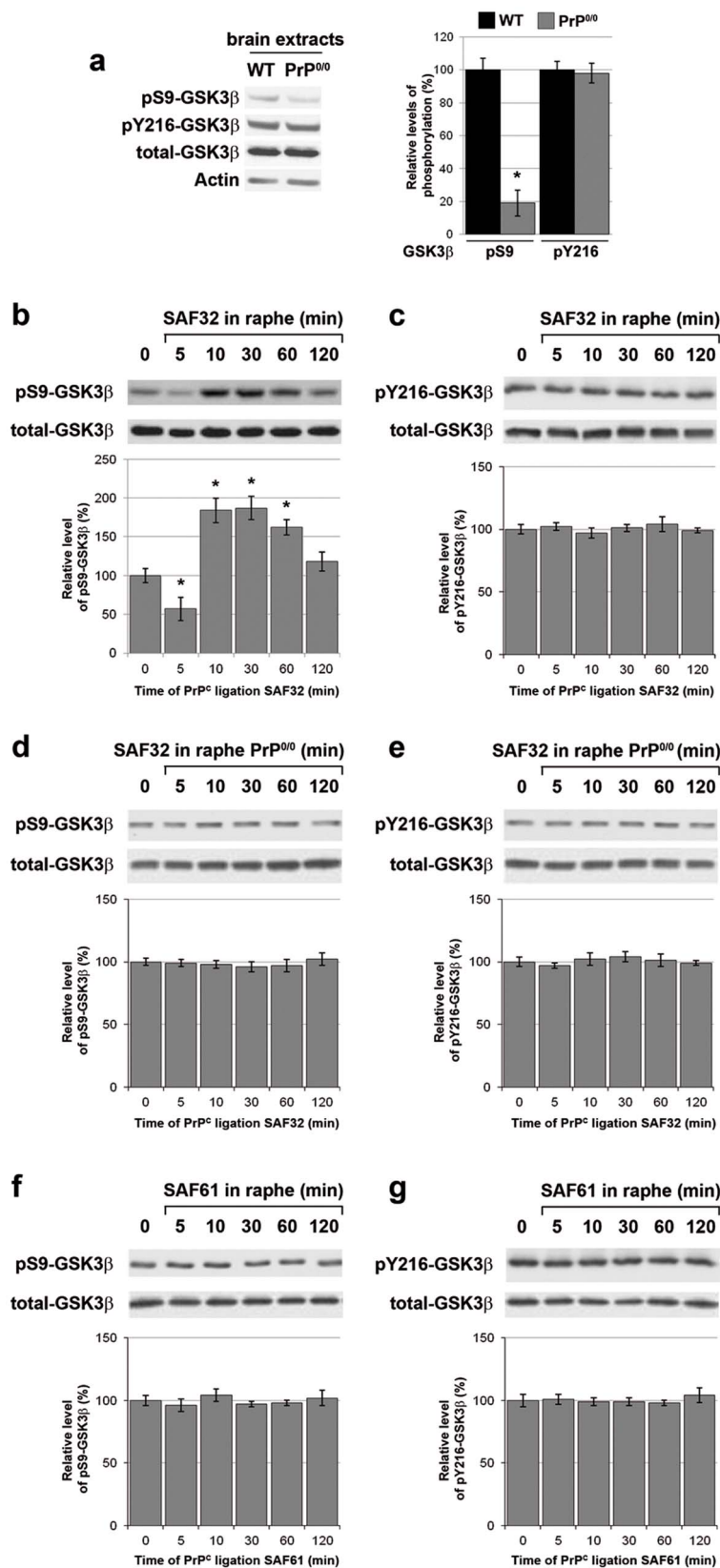
Figure 2 | PrP^C-negatively controls GSK3β in mouse brain. (a) The levels of pS9-GSK3β, pY216-GSK3β and total GSK3β were assessed by immunoblotting in brain extracts from PrP$^{0/0}$ mice versus WT mice. Actin was used as loading control. Data are representative of n = 4 animals. (b–g) SAF32 (b–e) or SAF61 (f–g) anti-PrP^C antibodies (2 μl at 1 mg/ml) were stereotaxically injected in the raphe nuclei of WT (b), (c), (f), (g) or PrP$^{0/0}$ mice (d), (e). Mice were sacrificed at the indicated time to collect raphe nuclei samples. The levels of pS9-GSK3β (b), (d), (f) or pY216-GSK3β (c), (e), (g) were assessed by immunoblotting of the raphe extracts and normalized to total GSK3β for quantification. Data are representative of n = 4 animals. Gels have been cropped for clarity and conciseness purposes and have been run under the same experimental conditions. Results are expressed as means ± S.E.M. *$P < 0.05$ vs. control, Kolmogorov-Smirnov test.
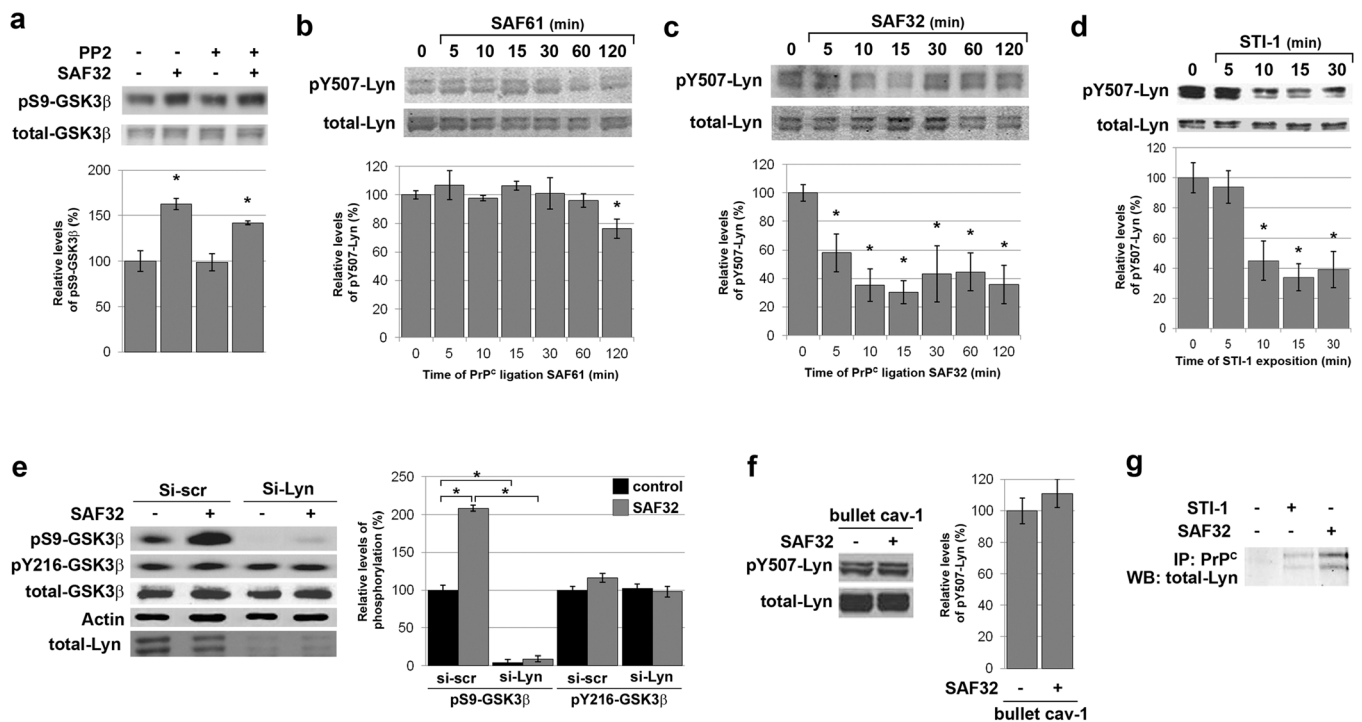
Figure 3 | PrP^C-mediated GSK3β phosphorylation on S9 is relayed by the Lyn kinase in 1C11^5-HT neuronal cells. (a) 1C11^5-HT neuronal cells were pre-incubated with the Fyn inhibitor PP2 (50 pM, 1 h) prior to exposure to SAF32 anti-PrP^C antibodies (10 μg/ml, 30 min), targeting native PrP^C. Cell lysates were immunoblotted with antibodies targeting pS9-GSK3β and total GSK3β for normalization. (b–d) 1C11^5-HT neuronal cells were exposed to anti-PrP^C antibodies targeting (b) a C-terminal epitope (SAF61, 10 μg/ml), (c) a N-terminal epitope (SAF32, 10 μg/ml) or (d) to a peptide corresponding to the domain of STI-1 that binds PrP^C (aa 230–245) (25 μM). Cell lysates were immunoblotted with antibodies targeting pY507-Lyn and total Lyn for normalization. (e) 1C11^5-HT neuronal cells were transfected for 36 h with a siRNA targeted against Lyn (Si-Lyn) or a control scramble siRNA (Si-scr) prior to exposure to SAF32 anti-PrP^C antibodies (30 min). Cell lysates were immunoblotted with antibodies targeting pS9-GSK3β, pY216-GSK3β, total GSK3β. Total Lyn was used to check knockdown and actin was used as loading control. (f) 1C11^5-HT neuronal cells were submitted to caveolin-1 immunosequestration prior to exposure to SAF32 antibodies (10 μg/ml, 15 min). Cell lysates were immunoblotted with antibodies against pY507-Lyn and total Lyn for normalization. (g) 1C11^5-HT neuronal cells were exposed to the STI-1 peptide (25 μM) or SAF32 antibodies (10 μg/ml) for 30 min. Cell lysates were immunoprecipitated with SAF61 anti-PrP^C antibodies and immunoblotted with antibodies against Lyn. Gels have been cropped for clarity and conciseness purposes; original images corresponding to (b–c) are shown in Supplemental Figure 5. Data are expressed as means ± S.E.M of n = 4 to 6 independent analyses. *$P < 0.05$ vs. control, Kolmogorov-Smirnov test.

cillamine (DPEN) abrogated the decrease in pY507-Lyn as well as the increases in pY458-p85-PI3K and in pS9-GSK3β induced by PrP^C ligation with SAF32 antibodies in 1C11^5-HT neuronal cells (Fig. 5f–h). These data indicate that the PrP^C-Lyn-PI3K-GSK3β cascade is copper-dependent and further support an involvement of full-length PrP^C since N-truncated PrP^C isoforms cannot bind copper.

The above results prompted us to further examine a potential involvement of the low density lipoprotein-related protein 1 (LRP1), a transmembrane protein that interacts with the N-terminal domain of PrP^C when it is copper bound[21,22]. To test whether LRP1 contributes to the PrP^C-Lyn-PI3K-GSK3β cascade, 1C11^5-HT neuronal cells were treated with the selective binding protein RAP, which blocks the interactions between LRP1 and its partners, including PrP^C. In resting conditions, addition of RAP triggered a strong increase in pY507-Lyn (276%) (Fig. 5f), suggesting that endogenous LRP1-partners interactions activate Lyn. Intriguingly, antibody-mediated ligation of PrP^C (SAF32) retained the capacity to promote a dephosphorylation of Lyn at Y507 in RAP-pre-treated cells (67%) (Fig. 5f), indicating that the interaction of PrP^C with LRP1 is not essential for recruitment of the Lyn kinase by PrP^C. In contrast, RAP cancelled the phosphorylation of p85-PI3K at Y458 and that of GSK3β at S9 promoted by SAF32 antibodies (Fig. 5g,h). Similar results were obtained upon siRNA-mediated silencing of LRP1 (data not shown). Thus, we may conclude that the PrP^C-LRP1 interaction is necessary for Lyn to relay the SAF32-mediated activation of the PI3K-Akt module and downstream inactivation of GSK3β.

The PrP^C-GSK3β coupling affects the distribution and negatively regulates the activity of the serotonin 1B receptor in 1C11^5-HT neuronal cells. An emerging substrate of the GSK3β kinase is the serotonergic 1B receptor (5-HT_{1B}R)[23], an autoreceptor that controls serotonergic functions and notably reduces serotonin (5-HT) release[24]. Blockade of GSK3β activity was shown to decrease the cell surface location of 5-HT_{1B}R and thereby its functionality in HEK293 cells[23,25]. On 1C11^5-HT serotonergic cells, the 5-HT_{1B}R is present and functional (negative coupling to adenylate cyclase)[26]. To test whether the 5-HT_{1B}R may be a target of the PrP^C-GSK3β coupling in 1C11^5-HT serotonergic cells, we assessed the impact of the PrP^C-dependent regulation of GSK3β activity on the subcellular distribution and activity of the 5-HT_{1B}R. Our experiments were designed to concomitantly monitor 5-HT_{1B}R numbers and activity in relation with their subcellular (i.e. cell bodies versus neurites) location. In untreated 1C11^5-HT serotonergic cells, we found that 81% of 5-HT_{1B}Rs were distributed in neurites and the remaining 19% in the cell bodies. Exposure of 1C11^5-HT neuronal cells to SAF32 antibodies, prior to cell fractionation, did not affect the global 5-HT_{1B}R protein level but reduced the pool of neuritic 5-HT_{1B}Rs to 41% and increased the cell bodies pool to 59% (Fig. 6a). As with SAF32 antibodies, the GSK3β inhibitors LiCl or SB216763 did not alter total 5-HT_{1B}R binding (Fig. 6a). When cells were treated with these drugs, the pool of 5-HT_{1B}Rs redistributed from the neurites (52% versus 81% in untreated cells) to the cell bodies 5-HT_{1B}Rs (48% versus 19% in untreated cells). These data
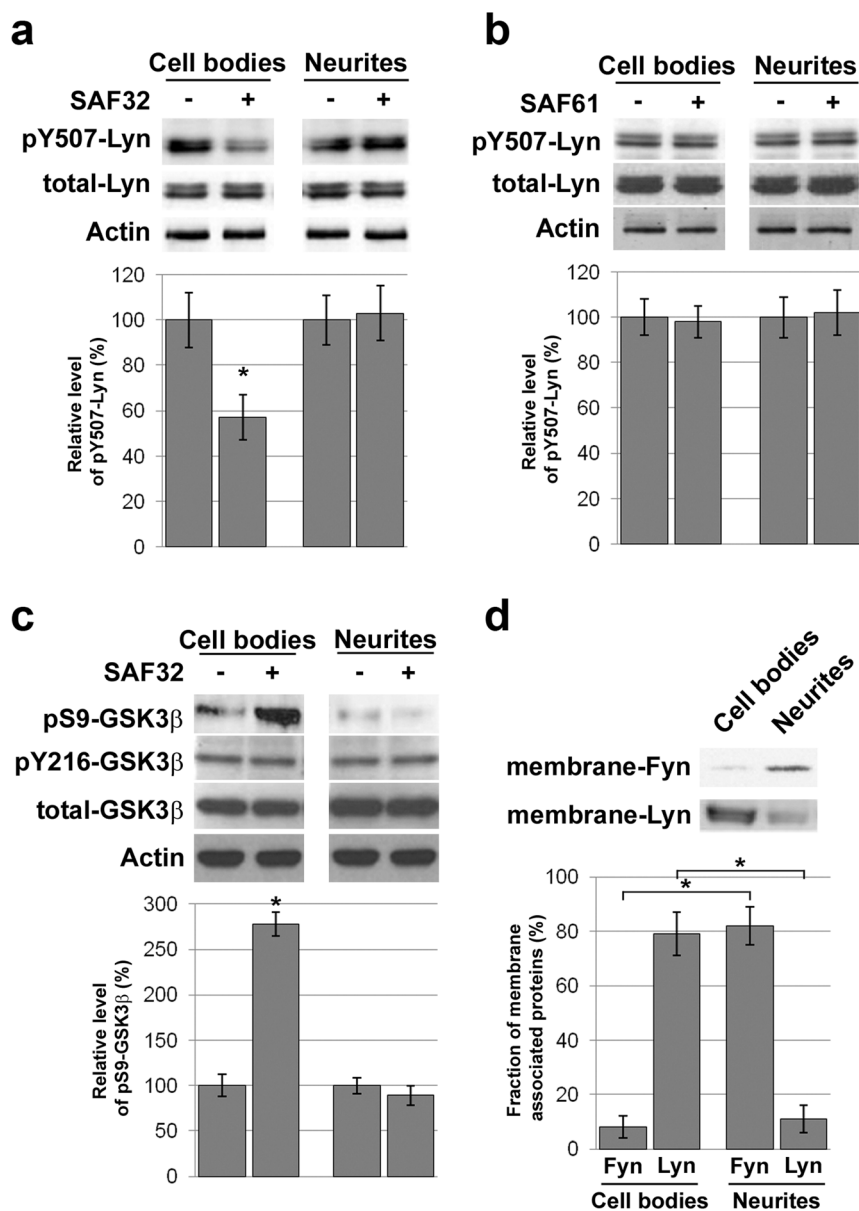
Figure 4 | The PrP^C-Lyn-GSK3β cascade involves PrP^C molecules located at the cell bodies of 1C11^{5-HT} neuronal cells. (a), (b) Cell bodies and neurites of 1C11^{5-HT} cells were separated prior exposure to SAF32 (a) or SAF61 (b) anti-PrP^C antibodies (10 μg/ml, 15 min). Lysates were immunoblotted with antibodies targeting pY507-Lyn or total Lyn. Actin was used as loading control. Cell fractionation was verified through immunoblotting with antibodies against lamin A/C, as shown in Supplemental Figure 6a. (c) pS9-GSK3β, pY216-GSK3β or total GSK3β levels were measured in cell bodies and neurites of 1C11^{5-HT} cells exposed to SAF32 anti-PrP^C antibodies (10 μg/ml, 30 min). Actin was used as loading control. (d) Membrane-associated Fyn and Lyn were quantified in cell bodies versus neurites of 1C11^{5-HT} cells. Membrane preparation was verified through immunoblotting with antibodies against NaK-ATPase, as shown in Supplemental Figure 6b. Gels have been cropped for clarity and conciseness purposes and have been run under the same experimental conditions. All data are representative of a set of n = 4 to 6 independent experiments. Results are expressed as means ± S.E.M. *$P < 0.05$ vs. control, Kolmogorov-Smirnov test.

thus indicate that the PrP^C-dependent inactivation of the GSK3β kinase affects the neurites versus cell bodies distribution of the 5-HT$_{1B}$R.

Next, we analyzed the functionality of the 5-HT$_{1B}$R in relation with its location (neurites versus cell bodies) by determining the inhibitory effect of the 5-HT$_{1B}$R agonist L694247 on 5-HT outflow. In control 1C11^{5-HT} serotonergic cells, both somatic and neuritic 5-HT$_{1B}$Rs could tone down 5-HT outflow (Fig. 6b). Somatic and neuritic 5-HT$_{1B}$Rs displayed similar activities towards 5-HT outflow in untreated 1C11^{5-HT} cells as inferred by the mean relative activity per binding site (Fig. 6c). Under SAF32- or drug-mediated inactivation of the GSK3β kinase, we monitored a drastic reduction in whole

cell 5-HT$_{1B}$R activity, revealed by a decrease in the inhibitory effect on 5-HT outflow (Fig. 6b). In these conditions, both 5-HT$_{1B}$Rs located in cell bodies or in neurites displayed little activity (Fig. 6b,c), indicating that GSK3β inactivation can quench both somatic and neuritic 5-HT$_{1B}$Rs activities (Fig. 6c).

Altogether, these results establish an antagonist role of PrP^C from cell bodies on global 5-HT$_{1B}$R activity via the GSK3β kinase and provide evidence for a potentiating effect of PrP^C on serotonergic neuronal activity.

The activity of the serotonin 1B receptor is increased in the substantia nigra of PrP$^{0/0}$ mice and its inhibition unleashes GABA and
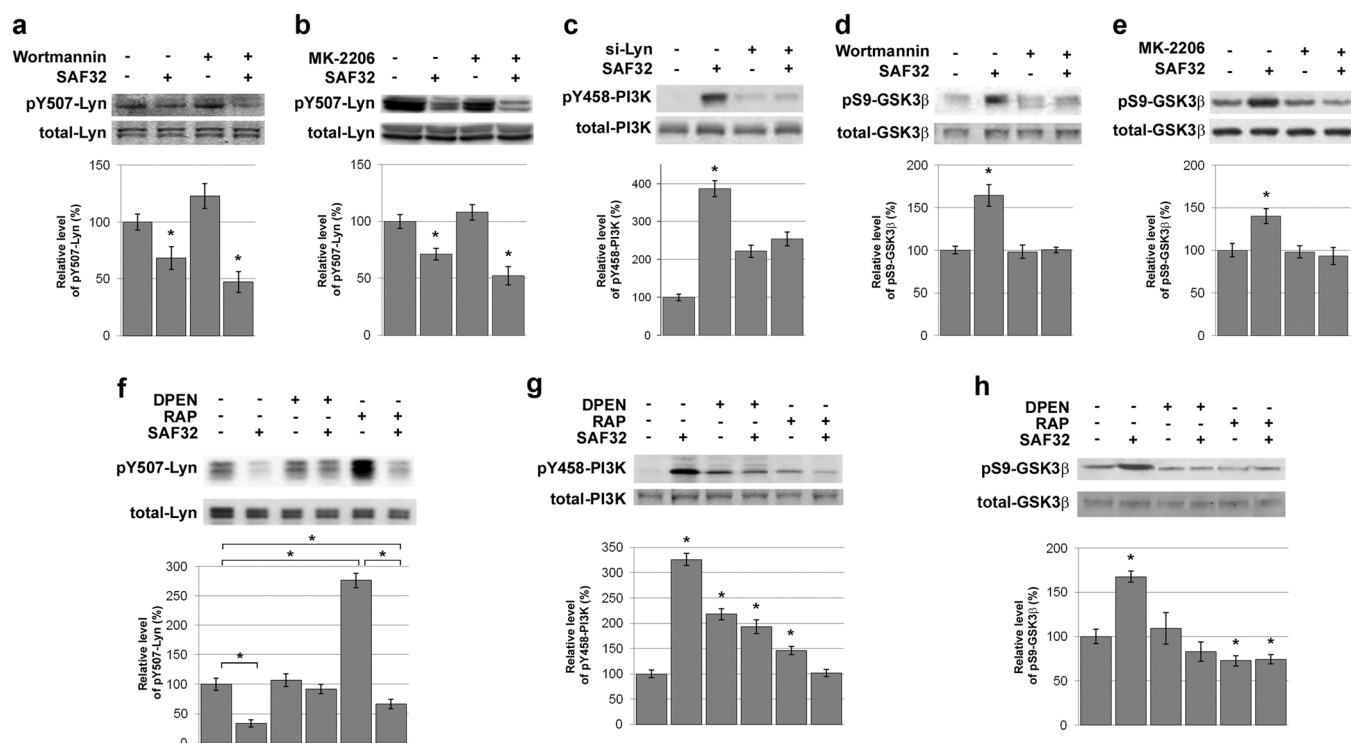
Figure 5 | The PrP^C-Lyn-GSK3β cascade in 1C11^{5-HT} neuronal cells is relayed by PI3K and Akt and involves copper and LRP1. (a), (b) 1C11^{5-HT} neuronal cells were pre-incubated for 1 h with the PI3K inhibitor Wortmannin (5 nM) (a) or the Akt Inhibitor MK-2206 (1 μM) (b), and then exposed to SAF32 anti-PrP^C antibodies (10 μg/ml, 15 min). Cell lysates were immunoblotted with antibodies targeting pY507-Lyn or total Lyn for normalization. (c) 1C11^{5-HT} neuronal cells were transfected for 36 h with a siRNA targeted against Lyn (Si-Lyn) or a control scramble siRNA prior to exposure to SAF32 anti-PrP^C antibodies. Cell lysates were immunoblotted with antibodies targeting pY458-p85 PI3K or total p85 PI3K. (d), (e) 1C11^{5-HT} neuronal cells were pre-incubated for 1 h with the PI3K inhibitor Wortmannin (5 nM) (d) or the Akt Inhibitor MK-2206 (1 μM) (e) prior to exposure to SAF32 anti-PrP^C antibodies (10 μg/ml, 30 min). Cell lysates were immunoblotted with antibodies targeting pS9-GSK3β or total GSK3β for normalization. (f–h) 1C11^{5-HT} cells were incubated for 1 h with the copper chelator DPEN (0.1 μg/ml) or the LRP1 antagonist RAP (200 nM), prior to exposure to SAF32 antibodies. Cell lysates were immunoblotted with antibodies targeting pY507-Lyn (f), pY458-p85 PI3K (g), or pS9-GSK3β (h). Levels of phosphorylated proteins were normalized to total corresponding proteins. Gels have been cropped for clarity and conciseness purposes and have been run under the same experimental conditions. All data are representative of a set of n = 4 to 6 independent experiments. Results are expressed as means ± S.E.M. *$P < 0.05$ vs. control, Kolmogorov-Smirnov test.

substance P releases and promotes an anxiogenic behavioural response. We further evaluated the in vivo relevance of the findings obtained with 1C11^{5-HT} serotonergic cells by assessing the number and functionality of 5-HT$_{1B}$Rs in PrP$^{0/0}$ versus WT mice. We focused on the substantia nigra, one of the brain regions where 5-HT$_{1B}$Rs are the most abundant[24]. Using [^{125}I]-GTI-binding to quantify these receptors, we measured a modest but significant (18%) increase in the number of 5-HT$_{1B}$Rs in PrP$^{0/0}$ mice as compared to WT mice (213 ± 15 versus 180 ± 12 fmoles/mg prot, respectively). Next, we evaluated the activity of this receptor in PrP$^{0/0}$ versus WT mice by studying the effect of the 5-HT$_{1B}$R antagonist SB224289 on KCl-evoked neurotransmitter release through in vivo microdialysis in awake mice (Fig. 7a). In agreement with[27], 5-HT release in the substantia nigra was barely sensitive to 5-HT$_{1B}$R inhibition (data not shown). Beyond serotonergic fibers, 5-HT$_{1B}$Rs in the substantia nigra are also found on GABAergic terminals where they act as heteroreceptors to downregulate GABA release[28]. We therefore measured the release of GABA evoked by KCl in PrP$^{0/0}$ versus WT mice, and assessed the impact of the 5-HT$_{1B}$R antagonist SB224289 on this response. In resting conditions, we measured similar basal GABA release in WT and PrP$^{0/0}$ mice. In the absence of SB224289, PrP$^{0/0}$ mice exhibited higher KCl-evoked GABA release than their WT counterparts. This observation can be accounted for by a 50% higher GABA content in the substantia nigra of PrP$^{0/0}$ versus WT mice (19.48 ± 1.68 versus 12.53 ± 0.91 nmoles/mg prot,

respectively, n = 6 animals, p < 0.05). As anticipated, SB224289 promoted a strong (270%) increase in KCl-evoked GABA release in WT mice. Of note, we measured a stronger potentiating effect of SB224289 on GABA release in PrP$^{0/0}$ mice (411%) (Fig. 7a), consistent with a sustained 5-HT$_{1B}$R activity in these mice.

Since substance P is frequently co-released with GABA in the substantia nigra[29], we further measured the levels of this neuropeptide in the dialysate samples. As for GABA, the levels of KCl-induced substance P release were higher in PrP$^{0/0}$ than WT mice (Fig. 7b). Interestingly, the potentiating effect of SB224289 on KCl-induced substance P release was also exarcebated in PrP$^{0/0}$ mice (307%) as compared to their WT counterparts (239%), with substance P levels reaching 253% of those measured in WT mice (Fig. 7b).

We finally sought to assess the behavioural outcome of the exacerbated activity of the 5-HT$_{1B}$R in PrP$^{0/0}$ mice. First, in line with the elevated locomotor activity associated with activation of 5-HT$_{1B}$ receptors[30], we monitored an increase in the locomotor activity of PrP null mice vs WT controls in the open field test, (426 ± 33 versus 321 ± 27 cm per 5-min block, respectively, n = 5 animals, p < 0.05). Furthermore, because increased substance P produces anxiogenic-like responses[31], we tested PrP$^{0/0}$ mice in the elevated plus maze, a well-established paradigm to detect the variability of anxiety-like behaviours in rodents[32]. In basal conditions or after KCl injection alone in the substantia nigra, there was no significant difference in the behaviour of PrP$^{0/0}$ and WT mice in our paradigm (Fig. 7c–f). WT mice injected with both KCl and the 5-HT$_{1B}$R antagonist SB224289
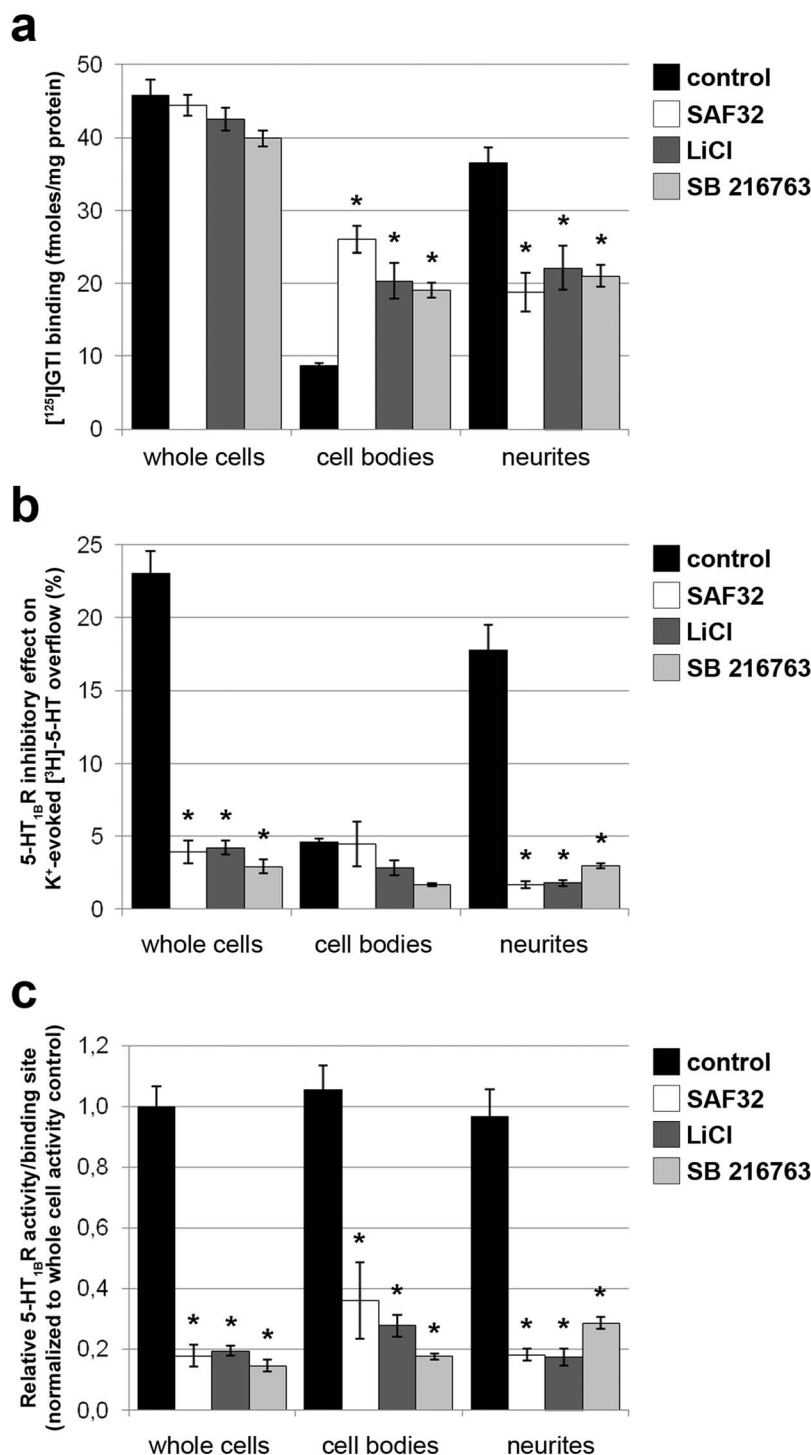
Figure 6 | The PrP^C-GSK3β cascade affects the subcellular distribution of the serotonin 1B receptor and negatively regulates its activity. (a) 1C11$^{5\text{-HT}}$ neuronal cells were exposed to SAF32 (10 μg/ml) anti-PrP^C antibodies or the GSK3β inhibitors LiCl (1 mM) or SB216763 (10 nM) for 30 min. 5-HT$_{1B}$Rs were quantified through [^{125}I]-GTI binding in whole cells and the corresponding cell bodies and neuritic fractions. (b) The 5-HT$_{1B}$R activity was determined by measuring the inhibitory effect of the 5-HT$_{1B}$R agonist L694247 on K$^+$-evoked [^{3}H]-5-HT overflow in whole cells. Experiments were repeated after cell fractionation in the corresponding cell bodies and neuritic fractions. (c) The relative 5-HT$_{1B}$R activity was calculated by normalizing the inhibitory effect on [^{3}H]-5-HT overflow to [^{125}I]-GTI binding for each pool of cells, both before and after cell fractionation. A total of n = 6 independent cultures were analyzed. Results are expressed as means ± S.E.M. *$P < 0.05$ vs. control, Kolmogorov-Smirnov test.

in the substantia nigra also adopted a behaviour that was similar to that of untreated or KCl-treated WT mice. In contrast, the injection of both KCl and SB224289 in PrP$^{0/0}$ mice drastically affected their behaviour. Indeed, these mice exhibited reduced frequency (Fig. 7c) and time (Fig. 7d) spent in open arms, and the overall distance

measured throughout the experiment was decreased (Fig. 7e). Further, the time spent in risk assessment was higher in KCl- and SB224289-treated PrP$^{0/0}$ mice than in their WT counterparts (Fig. 7f). The changes monitored with these four parameters reveal an anxiety-like behaviour in PrP$^{0/0}$ mice upon inhibition of the 5-HT$_{1B}$R.
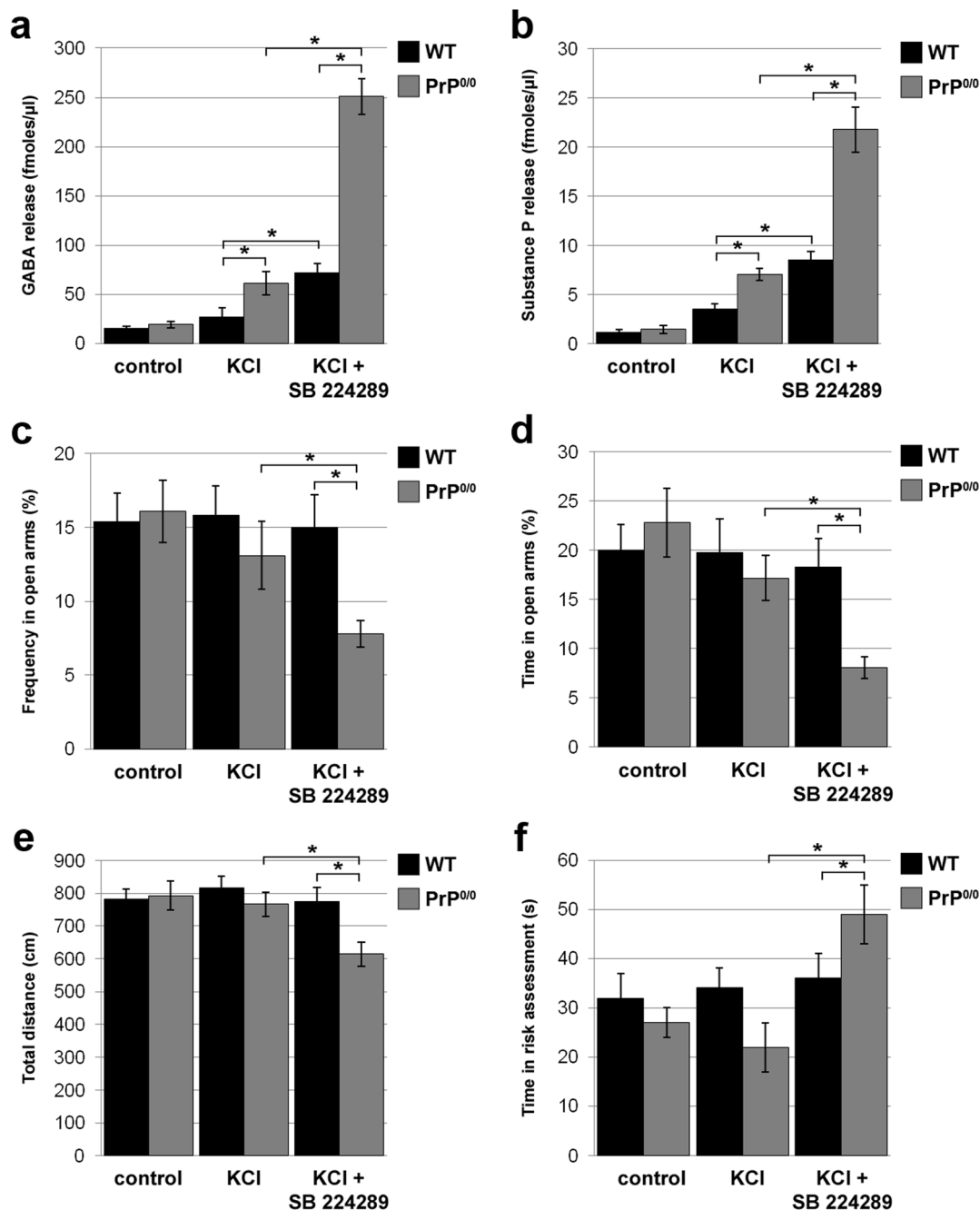
Figure 7 | Inhibition of serotonin 1B receptors in the substantia nigra of PrP-null mice unleashes GABA and substance P release and promotes an anxiogenic behavioural response. (a), (b) The effect of 5-HT$_{1B}$R inhibition on KCl-evoked GABA (a) and substance P (b) release was measured by in vivo microdialysis in awake WT and PrP$^{0/0}$ mice. In response to KCl alone, PrP$^{0/0}$ mice exhibited stronger GABA (a) and substance P (b) release than WT mice. 5-HT$_{1B}$R pharmacological inhibition (SB224289, 100 nM) exacerbated GABA (a) and substance P (b) release in WT animals. The potentiating effect of the 5-HT$_{1B}$R antagonist on GABA (a) and substance P (b) release was dramatically increased in PrP$^{0/0}$ mice. (c–f) The anxiety-like behaviour of PrP$^{0/0}$ versus WT mice was probed in the elevated plus maze. Three groups of each type of mice were tested: one group served as controls, a second group received a KCl injection (30 mM) in the substantia nigra and the last group received SB224289 (100 nM) prior to KCl injection. Mice were placed in the elevated plus maze 30 min after KCl treatment. Each trial was recorded for 5 min and further analysed to quantify frequency in open arms (c), time spent in open arms (d), total distance traversed (e) and time spent in risk assessment (f). Data are expressed as means ± S.E.M of n = 6 animals. *$P < 0.05$ vs. control, Kolmogorov-Smirnov test.

As a whole, we may conclude that PrP deficiency in mice is associated with a high increase in the activity of 5-HT$_{1B}$R in the substantia nigra, whose inhibition promotes exacerbated GABA and substance P releases together with an anxiogenic behavioural response. Thus, these results validate at an in vivo level the potentiating effect of the PrP^C-GSK3β coupling on neurotransmission through its inhibitory action on the 5-HT$_{1B}$ receptor.

Discussion

The present work introduces the GSK3β kinase as a new target of PrP^C-dependent cell signalling in neuronal cells. We show that native, i.e. full-length, PrP^C can trigger phosphorylation of the GSK3β kinase on S9 in 1C11$^{5\text{-HT}}$ serotonergic cells, which is associated with reduced GSK3β kinase activity. This signal, which can be monitored through antibody-mediated ligation of PrP^C, occurs in

response to the binding of PrP^C to its ligand STI-1 in 1C11$^{5\text{-HT}}$ as well as in PC12 neuronal cells. Conversely, depletion of PrP^C in 1C11$^{5\text{-HT}}$ cells correlates with decreased levels of pS9-GSK3β, highlighting an endogenous inhibitory action of PrP^C on GSK3β activity. We further confirmed that the activity of GSK3β is regulated by PrP^C in the brain, notably in serotonergic raphe (Fig. 2).

A current view is that PrP^C signalling is linked to the assembly of multicomponent complexes at the cell surface[33]. In agreement, our data demonstrate that the coupling to GSK3β is instigated by a PrP^C-cav-Lyn platform, that can be recruited after binding of PrP^C to its ligand STI-1. In this complex, native PrP^C is copper-bound and must associate with its transmembrane partner LRP1 to activate the PI3K-Akt module downstream from Lyn (see Fig. S3). This observation suggests that the recruitment of full-length, copper-bound PrP^C promotes its LRP1-dependent internalization[21]. Importantly, our findings substantiate a restriction of the PrP^C-Lyn-GSK3β coupling to the cell bodies of 1C11$^{5\text{-HT}}$ neuronal cells (Fig. 4). In the past, we reported that the PrP^C-caveolin-Fyn complex is selectively implemented on the neurites of fully-differentiated 1C11 neuronal cells, while all protagonists are present in both cell bodies and neurites[7]. Here, the spatial restriction of the PrP^C-Lyn-GSK3β signal cannot be accounted for by a specific distribution of intracellular effectors either, since Lyn and GSK3β were both found in the two compartments. We could further exclude a selective involvement of the membrane protein caveolin in the PrP^C coupling to Fyn on neurites since caveolin also serves as a relay in the PrP^C-Lyn cascade on cell bodies. Rather, our data argue that the implementation of the PrP^C-caveolin-Lyn platform on the cell bodies of 1C11$^{5\text{-HT}}$ neuronal cells arises from the selective association of somatic but not neuritic Lyn to the plasma membrane, to the opposite of Fyn. These data reinforce the idea that PrP^C-mediated signalling cascades are subject to tight spatial control driven by subsets of lipid raft microdomains[34,35].

GSK3β is an extremely pleiotropic kinase, that lies downstream of major signalling pathways including Wnt, Notch, insulin and growth factors[13]. GSK3β differs from most kinases in that it is active under resting conditions and is mostly regulated through inhibition[13]. Over a hundred substrates of GSK3β have been identified, with diverse roles in metabolism, cellular architecture, gene expression, neurodevelopment, axonal growth and polarity, neuronal/cellular survival[13]. Our findings that the interaction of PrP^C with STI-1 can trigger the neuroprotective inhibition of GSK3β is thus in agreement with the stress-protective role of STI-1[36] as well as with the notion that PrP^C acts as a gatekeeper against stress and confers resistance towards cellular insults[37,38]. Because GSK3β inhibition has been shown to play a pivotal role in synaptic plasticity and long-term potentiation (LTP)[39], our work also provides a molecular basis accounting for the involvement of the PrP^C-STI-1 duo in these processes[40]. Importantly, the interaction of STI-1 with PrP^C was recently shown to hinder the binding of Aβ oligomers to PrP^C and counteract their toxicity[41]. As suggested by the latter study, the inhibition of GSK3β downstream from STI-1-PrP^C evidenced here may further contribute to prevent Aβ-mediated toxic action.

The present study further provides evidence for an involvement of the PrP^C-GSK3β cascade in the control of serotonergic functions since PrP^C-dependent inhibition of GSK3β affects the serotonergic 5-HT$_{1B}$ receptor location and activity. As auto- or hetero-receptors, serotonin 5-HT$_{1B}$ receptors negatively regulate the release of serotonin and that of other neurotransmitters[24]. In serotonergic neurons, 5-HT$_{1B}$Rs globally tone-down serotonergic activity through combined reduction of 5-HT synthesis and release and enhanced uptake[42,43]. The 5-HT$_{1B}$R was recently shown to be a substrate for GSK3β-mediated phosphorylation, which enhances its activity[23]. The GSK3β-dependent regulation of the 5-HT$_{1B}$R also occurs in vivo since the selective depletion of GSK3β in serotonergic neurons was reported to compromise 5-HT$_{1B}$R-related neuronal firing, serotonin release and serotonin-regulated behaviors[44]. Here, we establish that

the PrP^C-dependent inactivation of GSK3β hinders the proper trafficking of the 5-HT$_{1B}$R and blunts its ability to reduce the outflow of serotonin induced by K$^+$-dependent depolarization in 1C11$^{5\text{-HT}}$ serotonergic cells (Fig. 6). By suppressing GSK3β activity and limiting 5-HT$_{1B}$R function, PrP^C thereby potentiates 5-HT transmission. This novel aspect of PrP^C signalling again fully fits in with our previous data supporting that PrP^C strengthens neuronal activity and provides a new connection between PrP^C and serotonergic functions[10,45].

Finally, our results at a cellular scale were recapitulated in vivo since we monitored increased GSK3β activity and 5-HT$_{1B}$R function in the brains of PrP$^{0/0}$ mice as compared to their WT counterparts. Of note, antagonizing the exacerbated 5-HT$_{1B}$R activity in the substantia nigra of PrP$^{0/0}$ mice promotes dramatic increases in GABA and substance P releases together with an anxiogenic behavioural response. These observations fit in with the well-established notion that the 5-HT$_{1B}$R negatively controls anxiety[46]. They are also reminiscent of several reports that PrP$^{0/0}$ mice exhibit reduced anxiety in various paradigms[47,48]. Interestingly, we previously documented that BSE-infected mice exhibited an anxiolytic-like behaviour similar to that of PrP$^{0/0}$ mice[48]. This phenotype would be thus consistent with increased GSK3β activity, in line with very recent data[49], and exacerbated 5-HT$_{1B}$R function. In view of the major role ascribed to GSK3β overactivation in neurodegeneration[50,51], whether restoring control on GSK3β activity in prion-infected neurons may help preserve brain neurotransmission deserves further investigation.

Methods

was performed by pretreating cells at 37°C for 1 h in their culture medium with the appropriate inhibitor prior to exposure to PrP antibody.

Preparation of cell extracts, co-immunoprecipitation, cell fractionation, membrane isolation. 1C11$^{5\text{-HT}}$ or PC12 cells were washed in PBS with 1 mM Ca^{2+} and Mg^{2+} and incubated for 30 min at 4°C in NaDOC lysis buffer [50 mM Tris·HCl (pH 7.4)/150 mM NaCl/5 mM EDTA/0.5% Triton X-100/0.5% sodium deoxycholate/1 mM Na_3VO_4 and a mixture of protease inhibitors, Roche, Mannheim, Germany]. Extracts were centrifuged at $14,000 \times g$ for 15 min and supernatants were stored at −80°C until use. Co-immunoprecipitation experiments were carried out as in[7]. Neurite/nerve growth cone fractions of 1C11$^{5\text{-HT}}$ cells were prepared according to[7]. To isolate membranes, fractions were resuspended in cold buffer containing 4 mM EDTA, 1 mM EGTA, 0.1 mM PMSF, 10 mM imidazole, pH 7.3. After centrifugation, the supernatant was poured onto a 20% sucrose cushion, and then centrifuged at 100,000 g for 90 min. The pellet containing the membrane fraction was used for further analysis. Protein concentrations were measured by using the bicinchoninic acid method (Pierce, Rockford, IL, USA).

Western blot analyses. Fifteen micrograms of proteins were resolved by 10% SDS-PAGE (Invitrogen) and transferred to nitrocellulose membranes (Amersham, Arlington Heights, IL, USA). Membranes were blocked with Odyssey blocking buffer (Li-Cor biosciences, Lincoln, NE, USA) for 1 h at room temperature and then incubated overnight at 4°C with primary antibody (1 μg/ml). Bound antibody was revealed by infrared detection using a secondary antibody coupled to IRDye fluorophores (Li-Cor biosciences). Western blot read out was performed with the Odyssey Infrared Imaging System (Li-Cor biosciences).

Immunofluorescence experiments. Cells grown on labtek chambers (Nunc, Rochester, NY, USA) were washed in PBS with 1 mM Ca^{2+} and Mg^{2+} (buffer A) and fixed with 4% formaldehyde in buffer A. Cells were then permeabilized with blocking buffer (buffer A with 20 mM Glycine, 1% goat serum and 0.1% Triton X-100) for 15 min at room temperature. Cells were next incubated with primary antibody (5 μg/ml) diluted in buffer A enriched with 1% goat serum and 0.1% Tween for 1 h at room temperature. Alexa Fluor 488 immunoglobulins (4 μg/ml) (Molecular Probes, Eugene, OR, USA) were used as secondary antibodies and 4′, 6-diamidino-2-phenylindole (Sigma-Aldrich, St. Louis, MO, USA) as nuclear marker. Immunolabelling was observed with a Nikon Eclipse TE2000-E inverted microscope (Nikon Instruments Inc., Melville, NY, USA) equipped with a black and white CCD CoolSnap HQ2 camera (Photometrics, Tucson, AZ, USA), controlled by NIS-element software (Nikon Instruments Inc.).

Stereotaxic injection of PrP^C antibodies. Stainless steel injectors were stereotaxically implanted into the raphe of avertin anaesthetized mice according to the mouse brain atlas of Paxinos and Franklin[55]. SAF32 or SAF61 antibodies (2 μl at 1 mg/ml) were injected into the raphe. Mice were decapitated at 5 to 120 min post-lesion, and the raphe were collected for protein extraction and analysis by western blot experiments.

Measurement of copper. Copper was measured by Zeeman electrothermal atomic adsorption spectrometry (ETAAS) on a SIMAA 6100 spectrometer (Perkin-Elmer, Courtaboeuf, France) using a 1 : 8 dilution of culture medium, as in[56].

5-HT$_{1B}$ receptor radioligand binding experiments. 5-HT$_{1B}$ receptors were detected using [^{125}I]-GTI in intact cells as in[26] or in brain samples as in[57]. Binding experiments were performed at room temperature, under shaking. Assays were initiated by the addition of 100 μl of fetal calf serum (FCS)-free DMEM containing 25 nM [^{125}I]-GTI. The specific binding was defined as the binding that was inhibited by 1 μM of homologous unlabeled ligand. A 30 min incubation period was followed by the addition of ice-cold Tris pH 7.4. Samples were filtered on polyethyleneimine-treated filters and radioactivity was counted in a γ scintillation counter (Packard, France). Experiments were performed both before and after cell fractionation of the same pool of cells to quantify 5HT$_{1B}$ receptors on the neurites and cell bodies fractions.

Measurement of serotonin overflow in 1C11$^{5\text{-HT}}$ neuronal cells. Cells were labeled with [^{3}H]-serotonin (1.3 μCi/ml) in Krebs buffer for 30 min at 37°C as in[44]. Cells were transferred into perfusion chambers and superfused at a flow rate of 0.5 ml per min. The superfusion fluid was collected beginning at 45 min of perfusion. Cells were stimulated with potassium chloride (KCl, 30 mM) at 50 min and then at 70 min in the presence of the 5-HT$_{1B}$R agonist L694247 (30 mM), added at 65 min. Collection of superfusion fluid was maintained until 90 min. Superfusion fluid from each fraction was mixed with scintillation liquid to count radioactivity in a β scintillation counter. The radioactivity from fractions collected at 51–53 min were averaged for the basal K+ evoked [^{3}H]-serotonin overflow and those from fractions collected at 71–73 min were averaged for the second K+ evoked [^{3}H]-serotonin overflow. The effect of the 5-HT$_{1B}$R agonist L694247 was determined by the ratio of the second overflow to the first overflow. Experiments were repeated after cell fractionation of the same pool of cells to calculate 5HT$_{1B}$R inhibitory effect on K+ evoked [^{3}H]-serotonin overflow on the neurites and cell bodies fractions.

Microdialysis. Anesthetized animals were placed in a stereotaxic frame and a stainless-steel guide cannula (CMA/12, CMA Microdialysis, North Chelmsford, MA, USA; outer diameter 0.7 mm) was implanted in the substantia nigra. According to Franklin and Paxinos[55], stereotaxic coordinates in mm for the substantia nigra were

3.0 posterior to the bregma, 1.3 lateral to the midline and 4.7 ventral to the surface of the skull. The cannula was then secured to the skull with dental cement, and the skin was sutured. Animals were kept in individual cages for a seven-day recovery. The microdialysis experiment was performed using awake mice. Dialysis probes were equipped with a Cuprophan membrane (membrane length 1 mm and diameter 0.24 mm, cutoff: 5,000 Da, Microdialysis AB, Sweden). Probes were perfused at a constant rate of 2 μl/min with artificial CSF containing 154.1 mM Cl−, 147 mM Na+, 2.7 mM K+, 1 mM Mg^{2+}, and 1.2 mM Ca^{2+}, adjusted to pH 7.4 with 2 mM sodium phosphate buffer. Dialysates were collected every 3 min over a 60 min period. KCl (30 mM) was injected 10 min after the beginning of the measurements. Mice received saline or SB224489 (100 nM) 5 min prior to KCl injection. Neurotransmitter release responses were averaged over the fractions collected at 11–14 min and 14–17 min. At the end of the experiment, all brains were fixed in a 4% formaldehyde solution and serial coronal slices were made on a microtome. Histological examination of cannula tip placement was subsequently made on 100 μm safranine-stained coronal sections. Dialysate samples were injected without any purification into an HPLC system that consists of a pump linked to an automatic injector (Agilent 1100, Palo Alto, CA, USA), a reverse-phase column (Zorbax SB C18, 3.5 lm, 150 · 4.6 mm; Agilent Technologies, Palo Alto, CA, USA) and a coulometric detector (Coulochem II; ESA Inc., Chelmsford, USA) with a 5011 analytical cell to quantify GABA. The first electrode was fixed at −100 mV and the second electrode at +300 mV. The gain of the detector was set at 50 nA. The signal of the second electrode was connected to an HP Chemstation for HPLC. The composition of the mobile phase was 50 mM NaH_2PO_4, 0.1 mM Na_2EDTA, 0.65 mM octyl sodium sulphate and 14% (v/v) methanol, pH 3.5. The flow rate was set at 1 ml/min. Substance P levels were measured in the microdialysates through radioimmunassay (Phoenix Pharmaceuticals Inc. Belmont, CA), according to manufacturer's instructions.

Behavioural tests. The locomotor activity was tested in a plexiglas open field (Med Associates, St Albans, VT, USA) and activity was monitored using the monitoring software (Med Associates, St Albans, VT, USA). Mice were allowed to habituate in the open field for 15 min, followed by the additional 30-min testing. Travel distances during each 5-min block were recorded. The elevated plus-maze (EPM) test was used because of its documented ability to readily detect the variability of anxiety-like behaviours in rodents[32]. The apparatus was composed of a central part (5 × 5 cm), two opposing open arms (27 × 5 cm) and two opposing enclosed arms (27 × 5 × 15 cm). The maze was made of black plexiglas, elevated at a height of 40 cm and the open arms were illuminated by two white bulbs providing a 30-lux illumination on their extremities. The test lasted 5 min and began with the placement of mice in the centre of the maze, facing an enclosed arm. A video camera mounted above the maze was used to record each trial and to allow a later analysis. The mice's reluctance to venture into the exposed open arms was taken as a measure of anxiety. This was indexed by the frequency of arm entries and time spent on the open arms: these measures were expressed as percentage scores over the total number of all (open and enclosed) arm entries, and total time spent in all arms, respectively. In addition, the total distance traversed in the entire maze surface was taken as a measure of general motor activity. We also assessed ethological measures of risk assessment (time spent in stretched-attend postures + time spent in flat-back approach) also reported to be relevant as an index of anxiety[58].

Statistics. The results are reported as the means ± standard errors of the means (S.E.M.). The non parametric Kolmogorov-Smirnov test were used for comparisons. A P-value < 0.05 was considered significant.

1. Aguzzi, A. & Calella, A. M. Prions: protein aggregation and infectious diseases. *Physiol Rev.* **89**, 1105–1152 (2009).
2. Larson, M. *et al.* The complex PrP(c)-Fyn couples human oligomeric Abeta with pathological tau changes in Alzheimer's disease. *J Neurosci* **32**, 16857–16871a (2012).
3. Lauren, J., Gimbel, D. A., Nygaard, H. B., Gilbert, J. W. & Strittmatter, S. M. Cellular prion protein mediates impairment of synaptic plasticity by amyloid-beta oligomers. *Nature.* **457**, 1128–1132 (2009).
4. Rambold, A. S. *et al.* Stress-protective signalling of prion protein is corrupted by scrapie prions. *EMBO J.* **27**, 1974–1984 (2008).
5. Roffe, M. *et al.* Prion protein interaction with stress-inducible protein 1 enhances neuronal protein synthesis via mTOR. *Proc Natl Acad Sci U S A* **107**, 13147–13152 (2010).
6. Zanata, S. M. *et al.* Stress-inducible protein 1 is a cell surface ligand for cellular prion that triggers neuroprotection. *EMBO J* **21**, 3307–3316 (2002).
7. Mouillet-Richard, S. *et al.* Signal transduction through prion protein. *Science* **289**, 1925–1928 (2000).
8. Schneider, B. *et al.* Understanding the neurospecificity of prion protein signaling. *Front Biosci.* **16**, 169–186 (2011).
9. Mouillet-Richard, S. *et al.* Regulation by neurotransmitter receptors of serotonergic or catecholaminergic neuronal cell differentiation. *J Biol Chem* **275**, 9186–9192 (2000).
10. Pradines, E. *et al.* CREB-dependent gene regulation by prion protein: impact on MMP-9 and beta-dystroglycan. *Cell Signal.* **20**, 2050–2058 (2008).
11. Grimes, C. A. & Jope, R. S. The multifaceted roles of glycogen synthase kinase 3beta in cellular signaling. *Prog Neurobiol.* **65**, 391–426 (2001).

12. Doble, B. W. & Woodgett, J. R. GSK-3: tricks of the trade for a multi-tasking kinase. *J Cell Sci* **116**, 1175–1186 (2003).

13. Kaidanovich-Beilin, O. & Woodgett, J. R. GSK-3: Functional Insights from Cell Biology and Animal Models. *Front Mol Neurosci* **4**, 40 (2011).

14. Salcedo-Tello, P., Ortiz-Matamoros, A. & Arias, C. GSK3 function in the brain during development, neuronal plasticity, and neurodegeneration. *Int J Alzheimers Dis* **2011**, 189728 (2011).

15. Feraudet, C. *et al.* Screening of 145 anti-PrP monoclonal antibodies for their capacity to inhibit PrPSc replication in infected cells. *J Biol Chem* **280**, 11247–11258 (2005).

16. Loberto, N. *et al.* The membrane environment of endogenous cellular prion protein in primary rat cerebellar neurons. *J Neurochem* **95**, 771–783 (2005).

17. Ingley, E. Functions of the Lyn tyrosine kinase in health and disease. *Cell Commun Signal* **10**, 21 (2012).

18. Sato, I. *et al.* Differential trafficking of Src, Lyn, Yes and Fyn is specified by the state of palmitoylation in the SH4 domain. *J Cell Sci* **122**, 965–975 (2009).

19. Vassallo, N. *et al.* Activation of phosphatidylinositol 3-kinase by cellular prion protein and its role in cell survival. *Biochem Biophys Res Commun.* **332**, 75–82 (2005).

20. Haigh, C. L., Marom, S. Y. & Collins, S. J. Copper, constitutive endoproteolytic processing of the prion protein and cell signalling. *Front Biosci.* **15**, 1086–1104 (2010).

21. Singh, I. *et al.* Low levels of copper disrupt brain amyloid-beta homeostasis by altering its production and clearance. *Proc Natl Acad Sci U S A* (2013).

22. Taylor, D. R. & Hooper, N. M. The low-density lipoprotein receptor-related protein 1 (LRP1) mediates the endocytosis of the cellular prion protein. *Biochem J.* **402**, 17–23 (2007).

23. Chen, L. *et al.* Glycogen synthase kinase-3beta is a functional modulator of serotonin-1B receptors. *Mol Pharmacol* **79**, 974–986 (2011).

24. Sari, Y. Serotonin1B receptors: from protein to physiological function and behavior. *Neurosci Biobehav Rev.* **28**, 565–582 (2004).

25. Chen, L., Salinas, G. D. & Li, X. Regulation of serotonin 1B receptor by glycogen synthase kinase-3. *Mol Pharmacol* **76**, 1150–1161 (2009).

26. Kellermann, O., Loric, S., Maroteaux, L. & Launay, J. M. Sequential onset of three 5-HT receptors during the 5-hydroxytryptaminergic differentiation of the murine 1C11 cell line. *Br J Pharmacol* **118**, 1161–1170 (1996).

27. Threlfell, S., Greenfield, S. A. & Cragg, S. J. 5-HT(1B) receptor regulation of serotonin (5-HT) release by endogenous 5-HT in the substantia nigra. *Neuroscience* **165**, 212–220 (2010).

28. Fink, K. B. & Gothert, M. 5-HT receptor regulation of neurotransmitter release. *Pharmacol Rev* **59**, 360–417 (2007).

29. Levesque, M., Wallman, M. J., Parent, R., Sik, A. & Parent, A. Neurokinin-1 and neurokinin-3 receptors in primate substantia nigra. *Neurosci Res* **57**, 362–371 (2007).

30. Cheetham, S. C. & Heal, D. J. Evidence that RU 24969-induced locomotor activity in C57/B1/6 mice is specifically mediated by the 5-HT1B receptor. *Br J Pharmacol* **110**, 1621–1629 (1993).

31. Ebner, K. & Singewald, N. The role of substance P in stress and anxiety responses. *Amino Acids* **31**, 251–272 (2006).

32. Pellow, S., Chopin, P., File, S. E. & Briley, M. Validation of open:closed arm entries in an elevated plus-maze as a measure of anxiety in the rat. *J Neurosci Methods* **14**, 149–167 (1985).

33. Linden, R. *et al.* Physiology of the prion protein. *Physiol Rev.* **88**, 673–728 (2008).

34. Lewis, V. & Hooper, N. M. The role of lipid rafts in prion protein biology. *Front Biosci.* **16**, 151–168 (2011).

35. Mishra, S. & Joshi, P. G. Lipid raft heterogeneity: an enigma. *J Neurochem* **103 Suppl 1**, 135–142 (2007).

36. Chiarini, L. B. *et al.* Cellular prion protein transduces neuroprotective signals. *Embo J.* **21**, 3317–3326 (2002).

37. Resenberger, U. K., Winklhofer, K. F. & Tatzelt, J. Neuroprotective and neurotoxic signaling by the prion protein. *Top Curr Chem* **305**, 101–119 (2011).

38. Roucou, X. & Leblanc, A. C. Cellular prion protein neuroprotective function: implications in prion diseases. *J Mol Med* **83**, 3–11 (2005).

39. Bradley, C. A. *et al.* A pivotal role of GSK-3 in synaptic plasticity. *Front Mol Neurosci* **5**, 13 (2012).

40. Coitinho, A. S. *et al.* Short-term memory formation and long-term memory consolidation are enhanced by cellular prion association to stress-inducible protein 1. *Neurobiol Dis.* **26**, 282–290 (2007).

41. Ostapchenko, V. G. *et al.* The prion protein ligand, stress-inducible phosphoprotein 1, regulates amyloid-beta oligomer toxicity. *J Neurosci* **33**, 16552–16564 (2013).

42. Hagan, C. E., McDevitt, R. A., Liu, Y., Furay, A. R. & Neumaier, J. F. 5-HT(1B) autoreceptor regulation of serotonin transporter activity in synaptosomes. *Synapse* **66**, 1024–1034 (2012).

43. Moret, C. & Briley, M. The possible role of 5-HT(1B/D) receptors in psychiatric disorders and their potential as a target for therapy. *Eur J Pharmacol.* **404**, 1–12 (2000).

44. Zhou, W. *et al.* The effects of glycogen synthase kinase-3beta in serotonin neurons. *PLoS One* **7**, e43262 (2012).

45. Mouillet-Richard, S. *et al.* Modulation of serotonergic receptor signaling and cross-talk by prion protein. *J Biol Chem* **280**, 4592–4601 (2005).

46. McDevitt, R. A. *et al.* Serotonin 1B autoreceptors originating in the caudal dorsal raphe nucleus reduce expression of fear and depression-like behavior. *Biol Psychiatry* **69**, 780–787 (2011).

47. Lobao-Soares, B. *et al.* Cellular prion protein regulates the motor behaviour performance and anxiety-induced responses in genetically modified mice. *Behav Brain Res* **183**, 87–94 (2007).

48. Vidal, C. *et al.* Early dysfunction of central 5-HT system in a murine model of bovine spongiform encephalopathy. *Neuroscience.* **160**, 731–743 (2009).

49. Simon, D. *et al.* Dysfunction of the PI3K-Akt-GSK-3 pathway is a common feature in cell culture and in vivo models of prion disease. *Neuropathol Appl Neurobiol* (2013).

50. Bhat, R. V. *et al.* Regulation and localization of tyrosine216 phosphorylation of glycogen synthase kinase-3beta in cellular and animal models of neuronal degeneration. *Proc Natl Acad Sci U S A* **97**, 11074–11079 (2000).

51. Hernandez, F. *et al.* The role of GSK3 in Alzheimer disease. *Brain Res Bull* **80**, 248–250 (2009).

52. Bueler, H. *et al.* Normal development and behaviour of mice lacking the neuronal cell-surface PrP protein. *Nature* **356**, 577–582 (1992).

53. Pantera, B. *et al.* PrPc activation induces neurite outgrowth and differentiation in PC12 cells: role for caveolin-1 in the signal transduction pathway. *J Neurochem* **110**, 194–207 (2009).

54. Schneider, B. *et al.* NADPH oxidase and extracellular regulated kinases 1/2 are targets of prion protein signaling in neuronal and nonneuronal cells. *Proc Natl Acad Sci U S A* **100**, 13326–13331 (2003).

55. Paxinos, G. & Franklin, K. B. J. (eds.). *The mouse brain in stereotaxic coordinates,* (Academic Press, 2001).

56. El Balkhi, S. *et al.* Relative exchangeable copper: a new highly sensitive and highly specific biomarker for Wilson's disease diagnosis. *Clin Chim Acta* **412**, 2254–2260 (2011).

57. Baudry, A., Mouillet-Richard, S., Schneider, B., Launay, J. M. & Kellermann, O. miR-16 targets the serotonin transporter: a new facet for adaptive responses to antidepressants. *Science* **329**, 1537–1541 (2010).

58. Rodgers, R. J. & Johnson, N. J. Factor analysis of spatiotemporal and ethological measures in the murine elevated plus-maze test of anxiety. *Pharmacol Biochem Behav* **52**, 297–303 (1995).

Acknowledgments

Author contributions

J.-M.L. and S.M.-R. designed the project. J.H.-R., S.M.-L., T.Z.H., E.P. and A.A.-B. performed experiments. J.H.-R., S.M.-L., T.Z.H., E.P., B.S., A.B., J.-M.L. and S.M.-R. analysed the data. J.-M.L. and S.M.-R. supervised the project and wrote the manuscript.

Additional information

Supplementary information accompanies this paper at http://www.nature.com/scientificreports

Competing financial interests: The authors declare no competing financial interests.

How to cite this article: Hernandez-Rapp, J. *et al.* A PrP^C-caveolin-Lyn complex negatively controls neuronal GSK3β and serotonin 1B receptor. *Sci. Rep.* **4**, 4881; DOI:10.1038/srep04881 (2014).